ACS APPLIED MATERIALS & INTERFACES

Research Article

Cite This: ACS Appl. Mater. Interfaces 2018, 10, 40001−40007

www.acsami.org

Interfacial TADF Exciplex as a Tool to Localize Excitons, Improve Efficiency, and Increase OLED Lifetime

Marco Colella,* Piotr Pander, Daniel de Sa Pereira, and Andrew P. Monkman

Physics Department, Durham University, South Road, Durham DH1 3LE, United Kingdom

Supporting Information

ABSTRACT: In this work, we employ a thermally activated delayed fluorescence (TADF) exciplex formed between the emissive layer (EML) host, 26DCzPPy, and the electron transport layer (ETL) 2,4,6-tris[3-(diphenylphosphinyl)phenyl]-1,3,5-triazine at the interface between the EML and the ETL to improve the stability and efficiency of a phosphorescence organic light-emitting diode based on Ir(dmpq)$_2$acac. We show that the presence of the TADF exciplex at the EML−ETL interface induces an efficient localization of the recombination zone, which is confined within the 5 nm thick EML. Furthermore, the TADF exciplex allows harvesting of the holes and electrons that piled up at the EML−ETL interface and transfers the resultant excited state energy to the phosphorescent emitter through Förster and/or Dexter energy transfer. This approach effectively improves the LT90 of devices from <1 min to 6 h by limiting recombination processes outside of the 5 nm EML.

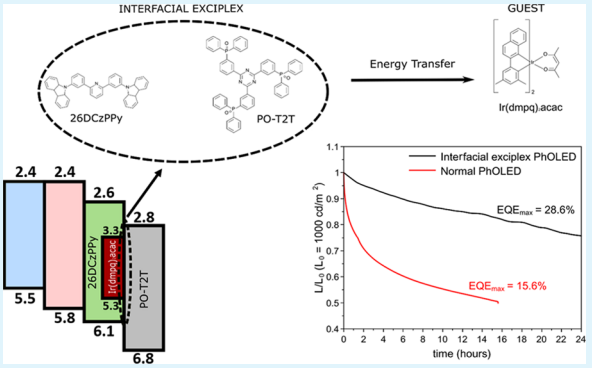

KEYWORDS: *OLED, PhOLED, TADF, exciplex, photophysics, FRET, DET*

INTRODUCTION

Since Tang and VanSlyke[1] reported the first efficient multilayer organic light-emitting diode (OLED), this field of research has grown extensively. Early research focused on finding a solution to the problem of harvesting all excitons produced by the electrical excitation where now it focuses on maximizing the fraction of emissive excited states because spin statistics dictate that in the OLED, through electrical excitation, only 25% of the excitons produced are singlets with the remaining 75% being triplets. In normal fluorescent emitters, only singlets are allowed to decay radiatively, leading to a huge loss of internal efficiency of the OLED devices. The first solution to this problem was found using organometallic complexes based on heavy metals like iridium (Ir) and platinum (Pt)[2] to produce phosphorescent OLEDs (PhOLEDs). In these compounds, the singlets are converted into triplets via intersystem crossing (ISC), which then can efficiently decay radiatively due to the spin−orbit coupling induced from the presence of the heavy metal in the compound. The second solution for harvesting all electrically produced excited states is via thermally activated delayed fluorescence (TADF).[3] In this case, triplets can be upconverted to singlets via reverse-ISC (rISC) and emit via normal fluorescence. The rISC becomes efficient when the local excitonic triplet (^{3}LE) and the charge-transfer triplet state (^{3}CT), formed between a donor (D) and an acceptor (A) unit, are vibronically coupled,[4] mediating the upconversion rISC of the ^{3}LE to the charge-transfer singlet state (^{1}CT). The same photophysical mechanism applies to both intra- and intermolecular CT states.[5] The latter case is also called an exciplex state when the CT state is formed between two different molecules. Efficiencies higher than 20% have been achieved with both approaches but when considering a more practical application, research in OLEDs aims not only for efficiency but also for small efficiency roll-off and long operational lifetime. Kondakova et al. in 2008 first reported on the performance enhancement of PhOLEDs when an exciplex cohost is employed.[6] Later, after Fukagawa et al.[7] demonstrated performance enhancement of PhOLEDs when a TADF host was used, many other groups also published using either TADF small molecules or exciplexes as hosts due to the effective Förster resonant energy transfer (FRET) to the emitter that these systems can provide, jointly with the 100% triplet harvesting via the TADF mechanism.[8−16] Furthermore, Duan et al.[13] demonstrated that by inserting a TADF exciplex at the interface between the host and the hole transport layer (HTL) of a PhOLED, it is possible to enhance the stability and the performance of the device exploiting the energy transfer from the interfacial exciplex and the guest material.

In this work, we investigated the effect of using such a strategy on the electron side of the device to improve the charge balance of the devices. The electron mobility in the OLED devices is indeed commonly lower than the hole mobility, causing the holes to pile up at the interface between the emissive layer (EML) and electron transport layer (ETL),

Received: September 19, 2018
Accepted: November 1, 2018
Published: November 1, 2018

DOI: 10.1021/acsami.8b15942
ACS Appl. Mater. Interfaces 2018, 10, 40001−40007

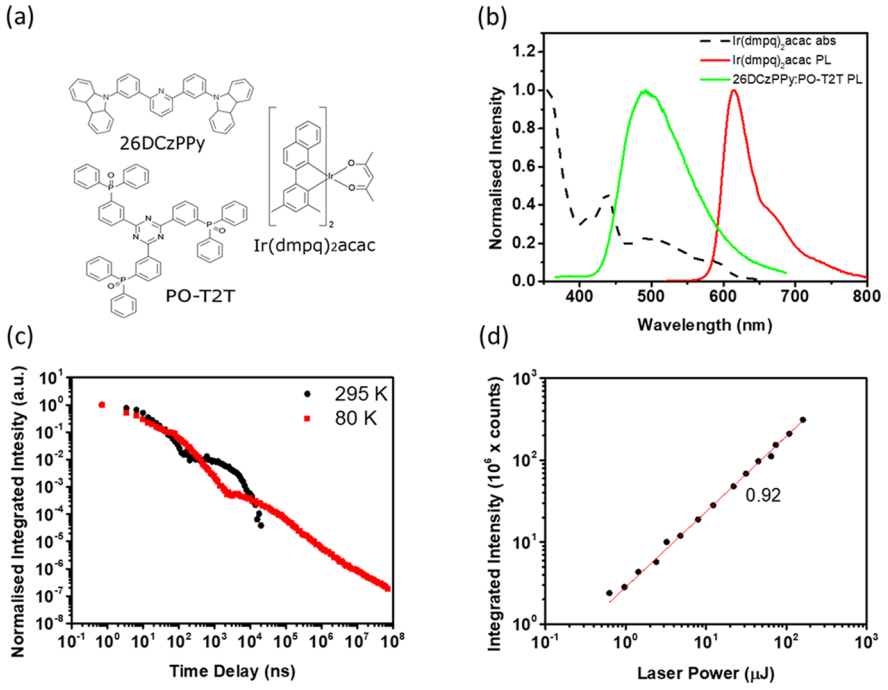

Figure 1. (a) Molecular structure of the exciplex forming donor (26DCzPPy), acceptor (PO-T2T), and phosphorescent emitter ($Ir(dmpq)_2acac$) used in this study. (b) The normalized absorption and photoluminescence (PL) spectra of Ir(dmpq)2acac and 26DCzPPy:PO-T2T exciplex. (c) Time-resolved fluorescence decay curves at 80 and 295 K. (d) Integrated area as a function of the laser excitation (355 nm) of 26DCzPPy:PO-T2T exciplex blend.

which could well be a source of device degradation. To address this problem, a TADF exciplex formed by the well-known bipolar EML host 2,6-bis[3-(9*H*-carbazol-9-yl)phenyl]pyridine (26DCzPPy) and the donor 2,4,6-tris[3-(diphenylphosphinyl)-phenyl]-1,3,5-triazine (PO-T2T) used as ETL, was introduced to avoid the pile-up problem. All devices were doped with bis(2-(3,5-dimethylphenyl)quinoline-*C*2,*N*′)(acetylacetonato)-iridium(III) ($Ir(dmpq)_2acac$) to obtain efficient FRET from the interfacial exciplex due to the extensive overlap of the absorption spectrum of the dopant with the exciplex emission as well as yield of 100% phosphorescent emission. The molecular structure of the molecules involved in the FRET process is shown in Figure 1a. Furthermore, we have employed device architecture with a 5 nm thick emissive layer (EML) that allowed us to assess the localization of the recombination zone and obtain more information about the energy-transfer mechanisms between the exciplex and the dopant. We were indeed able to observe when exciton localization was lost simply by observing the changes in the electroluminescence (EL) spectrum and relating those changes to the variations in the stability of the device with the different device structures.

A maximum external quantum efficiency (EQE) of 28.6% at 100 cd/m^2, as well as a very low roll-off with an efficiency of 25.2% at 1000 cd/m^2, was achieved using this architecture. Further device structures were used introducing a 1 nm spacer layer between the EML and the exciplex and by substituting PO-T2T alternatively with 2,2′,2″-(1,3,5-benzinetriyl)-tris(1-phenyl-1-*H*-benzimidazole) (TPBi) and 2,9-dimethyl-4,7-diphenyl-1,10-phenanthroline (BCP) to access the role of energy transfer to the $Ir(dmpq)_2acac$. All results highlight the importance of the energy-transfer process from the interfacial exciplex to the phosphorescent guest in the enhancement of both performances and stability of the devices.

METHODS

The OLEDs from this study were fabricated on a patterned indium tin oxide (ITO)-coated glass (Ossila) with a sheet resistance of 20 Ω/sq and ITO thickness of 100 nm. After loading the precleaned substrates into a Kurt J. Lesker Spectros II deposition chamber, both small molecules and cathode layers were thermally evaporated with a pressure of no more than 10^{-6} mbar for a pixel size of 4.5 mm^2. The devices produced were then encapsulated using UV-curable epoxy (DELO Katiobond) alongside the edges of the active area with a glass coverslip (Ossila). The materials used for the production of the devices were *N*,*N*′-di(1-naphthyl)-*N*,*N*′-diphenyl-(1,1′-biphenyl)-4,4′-diamine (NPB) and 4,4′,4″-tris(carbazol-9-yl)triphenylamine (TCTA), used, respectively, as a hole injection layer and hole transporting layer (HTL). 2,4,6-Tris[3-(diphenylphosphinyl)phenyl]-1,3,5-triazine (PO-T2T), 2,2′,2″-(1,3,5-benzinetriyl)-tris(1-phenyl-1-*H*-benzimidazole) (TPBi), and 2,9-dimethyl-4,7-diphenyl-1,10-phenanthroline (BCP) were used as an electron transport layer (ETL), whereas lithium fluoride (LiF) and aluminum (Al) were used as an electron injection layer and cathode, respectively. The 2,6-bis[3-(9*H*-carbazol-9-yl)phenyl]pyridine (26DCzPPy) was used as host material, and bis(2-(3,5-dimethylphenyl)quinoline-*C*2,*N*′)(acetylacetonato)-iridium(III) ($Ir(dmpq)_2acac$) as the emitting guest material. NPB, TCTA, BCP, and TPBi were purchased from Sigma-Aldrich and sublimed before being used for the production of OLEDs. 26DCzPPy, $Ir(dmpq)_2acac$ and PO-T2T were purchased, respectively, from Ossila and Lumtec and used as received. Steady-state absorption and emission spectra were acquired using a UV-3600 Shimadzu spectrophotometer and a Jobin Yvon Horiba Fluoromax-3 fluorometer, respectively. Time-resolved spectra were obtained by exciting the sample with a Nd:YAG laser (EKSPLA), 10 Hz, 355 nm. Sample emission was detected with a gated iCCD camera (Stanford Computer Optics).

RESULTS AND DISCUSSION

26DCzPPy:PO-T2T Photophysics. Although the 26DCzPPy:PO-T2T exciplex has been previously reported,[17] there has been little explanation to its photophysics. First of all,

DOI: 10.1021/acsami.8b15942
ACS Appl. Mater. Interfaces 2018, 10, 40001−40007

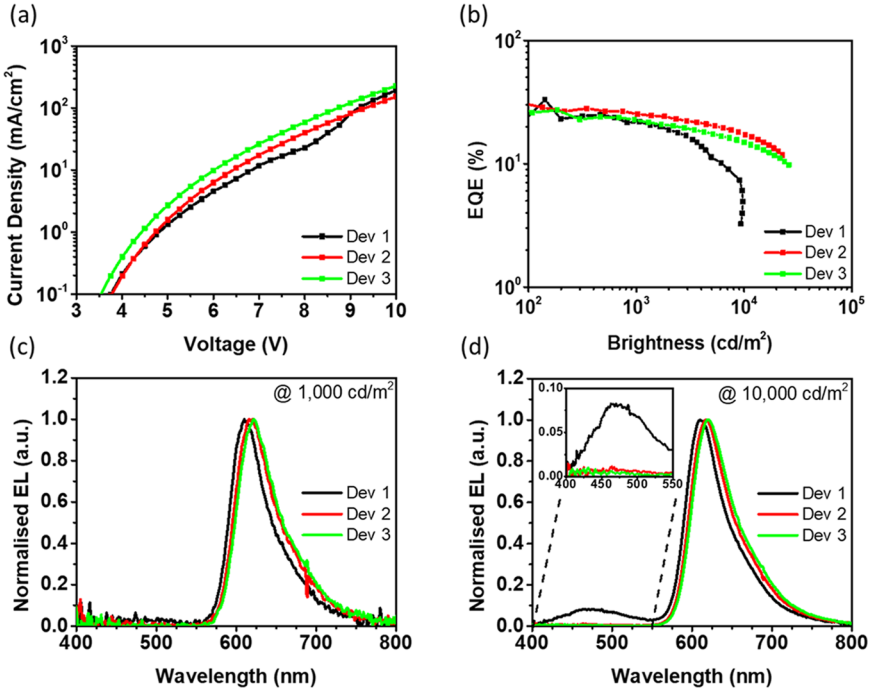

Figure 2. (a) *JV* and (b) EQE curves of the PhOLEDs with different doping levels of Ir(dmpq)2acac. Normalized EL spectra of the PhOLEDs at constant brightness of (c) 1000 cd/m^2 and (d) 10 000 cd/m^2.

the exciplex photoluminescence (PL) decay at room temperature (Figure 1c) is biexponential with prompt fluorescence (PF) decay time (τ_{PF} = 14.4 ± 0.4 ns) and delayed fluorescence (DF) decay time (τ_{DF} = 3.0 ± 0.2 μs). From the integral of the PF and DF regions of the PL decay (Figure S1), the ratio between the DF and PF contribution to the emission has been calculated (DF/PF ≈ 2.5) whereas the rISC rate is 1.1 × 10^6 s^{-1} calculated accordingly to the procedure published by Dias et al.[18] The singlet−triplet gap is estimated to be ΔE_{ST} = 0.09 eV. The delayed fluorescence changes its intensity with temperature, as observed from exciplex photoluminescence decay between 295 and 80 K in Figure 1c, which indicates a thermally activated character. Furthermore, the delayed fluorescence component shows a laser fluence dependency with a 0.92 exponent (Figure 1d). This being close to 1, a linear relation, along with the strongly temperature-dependent delayed fluorescence in Figure 1c, indicates the TADF mechanism to be the main triplet harvesting mechanism involved (i.e., excluding triplet−triplet annihilation).

Interestingly, the prompt and delayed fluorescence spectra of the exciplex blend are clearly distinct (Figure S2). The early emission spectrum at 0.7 ns delay shows the emission maximum at ≈460 nm, whereas at later time delays, there is a gradual redshift observed and the delayed fluorescence shows a maximum at ≈490 nm, as for the steady-state PL spectrum shown in Figure 1b. This behavior indicates significant structural geometry reorganization within the D and A molecules resulting in the charge-transfer (CT) emissive state energy relaxation. The TADF emission clearly dominates at 295 K, but at 80 K, a weak delayed fluorescence (1−100 μs delay) is accompanied by phosphorescence emission (>10 ms delay) of 26DCzPPy (see Figure S2).[19] This observation suggests that the local triplet state (^{3}LE) of 26DCzPPy is coupled with the exciplex charge-transfer (CT) state and the coupling of ^{1}CT and ^{3}CT with the ^{3}LE gives rise to TADF in this system. Figure 1b shows the extensive overlap between the absorption of Ir(dmpq)$_2$acac and the 26DCzPPy:PO-T2T PL, which is necessary to provide efficient FRET between the exciplex and the phosphorescent emitter.

PhOLEDs. Initially, we optimized the concentration of the dopant by implementing a device structure of NPB (40 nm)| TCTA (10 nm)|26DCzPPy (5 nm)|1−4−10 wt % of Ir(dmpq)$_2$acac in 26DCzPPy (5 nm)|PO-T2T (50 nm)|LiF (1 nm)|Al (100 nm), which are, respectively, labeled as Dev 1, Dev 2, and Dev 3. The 5 nm buffer layer of 26DCzPPy was used to avoid direct injection of holes from the TCTA layer into Ir(dmpq)$_2$acac to maximize the charge recombination at the exciplex interface and therefore to help the energy-transfer process from the interfacial exciplex to the guest phosphor to dominate the device physics. The slight redshift observed with the increased doping concentration in Figure 2c is due to reabsorption of the emitter emission. In fact, the emission and the absorption spectrum overlap in the region between 550 and 650 nm, showing a rather small Stokes shift, as visible in Figure 1b. In Figure 2a, it can be seen that the current density of the devices increases with the concentration of Ir(dmpq)$_2$acac in the EML. This is a typical behavior in PhOLEDs due to charge trapping on the iridium complexes since they act as deep traps for both holes and electrons.[20] The energy differences between the highest occupied molecular orbital and lowest unoccupied molecular orbital (LUMO) levels of 26DCzPPy and Ir(dmpq)$_2$acac are 0.61 and 0.74 eV, respectively.[10,21,22] In terms of efficiency, we find the device loaded with 4 wt % Ir(dmpq)$_2$acac, Dev 2, to exhibit the highest EQE at both reference brightness of 100 and 1000 cd/m^2 as 28.6 and 25.2%, respectively. We attribute this small roll-off to triplet−polaron quenching.[23] In general, all three devices show an efficiency roll-off of only 10% between 100 and 1000 cd/m^2. Interestingly, the device with 1 wt % Ir(dmpq)$_2$acac, Dev 1, shows performances similar to those of the device with 10 wt % Ir(dmpq)$_2$acac, Dev 3, up to the brightness of 2000

DOI: 10.1021/acsami.8b15942
ACS Appl. Mater. Interfaces 2018, 10, 40001−40007

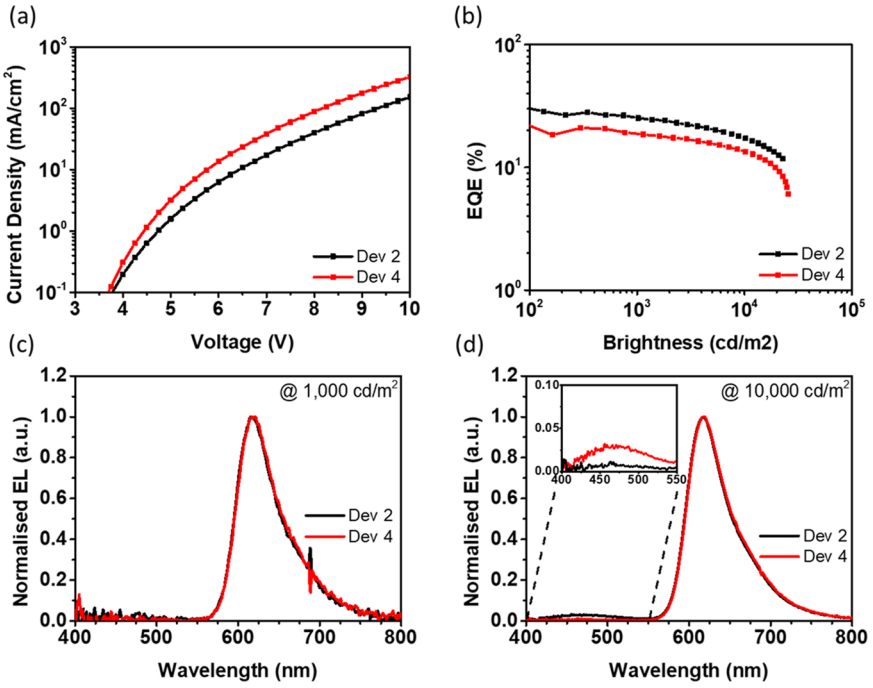

Figure 3. (a) *JV* and (b) EQE curves of the PhOLEDs with and without the 1 nm 26DCzPPy spacer layer at the EML|ETL interface. EL spectra of the PhOLEDs at constant brightness of (c) 1000 cd/m^2 and (d) 10 000 cd/m^2.

Table 1. Summary of the PhOLED Performances at Different Doping Levels

	@100 cd/m^2			@1000 cd/m^2			
wt % Ir(dmpq)$_2$acac	*V*	cd/A	EQE	*V*	cd/A	EQE	LT90 (h)
Dev 1—1 wt %	4.3	29.8 ± 9.1	24.5 ± 1.2	5.8	31.5 ± 0.9	21.9 ± 1.1	0.02
Dev 2—4 wt %	4.3	36.6 ± 6.6	28.6 ± 1.4	5.5	30.7 ± 0.8	25.2 ± 1.3	1
Dev 3—10 wt %	4.0	27.3 ± 4.5	26.0 ± 1.3	5.3	24.6 ± 0.5	22.7 ± 1.1	6
Dev 4—4 wt % 1 nm spacer	4.3	26.0 ± 2.7	18.4 ± 0.9	5.3	23.4 ± 0.4	18.6 ± 0.9	1
Dev 5—4 wt % TPBi	4.3	26.1 ± 3.9	15.6 ± 0.8	5.0	26.4 ± 0.5	21.3 ± 1.1	0.13
Dev 6—7 wt % BCP	5.5	21.4 ± 2.9	31.5 ± 1.6	7.0	15.3 ± 0.4	15.3 ± 0.8	>0.01

cd/m^2. Afterward, the efficiency drops significantly faster compared to that of the more heavily doped devices. This can be explained comparing the electroluminescence (EL) spectra shown in Figure 2c,d. The figures show the EL spectra at the same brightness of 1000 and 10 000 cd/m^2, respectively. No exciplex emission is visible in any of the devices at 1000 cd/m^2. However, in the spectra collected at brightness of 10 000 cd/m^2 (Figure 2d), Dev 1 shows a strong exciplex emission at 471 nm (inset of Figure 2d) whereas this was not visible in either Dev 2 or Dev 3. This observation confirms that the exciplex is indeed populated and that, even with a doping concentration as low as 1%, it can be fully harvested via FRET at a moderately low current density. We therefore interpret the abrupt EQE roll-off of Dev 1 at high current density to be the consequence of reaching the saturation of the energy-transfer process, which leads the exciplex peak to arise in the EL spectrum. The exciplex emission observed in the EL spectrum is blue-shifted by ≈20 nm from the PL spectrum of Figure 1b due to the interfacial geometry of the exciplex under the influence of the electric field in the OLED structure.[24] It should also be considered that the EML thickness is only 5 nm, which is within the typical triplet exciton diffusion length, making Dexter energy transfer (DET) from the 26DCzPPy–PO-T2T interface a non-negligible effect in this particular device structure, especially with the increment of doping concertation.[25]

To separate the contributions of DET and FRET to the energy-transfer process, we produced devices with a 1 nm spacer layer introduced between the EML and the PO-T2T. The device structure used is NPB (40 nm)|TCTA (10 nm)|26DCzPPy (5 nm)|4 wt % of Ir(dmpq)$_2$acac in 26DCzPPy (5 nm)|26DCzPPy (1 nm)|PO-T2T (50 nm)|LiF (1 nm)|Al (100 nm) labeled Dev 4. In Figure 3b, we see that the performance of Dev 4 is comparable to that of Dev 2 since both possess the same structure, differentiated only by the 1 nm spacer present in Dev 4. At 100 cd/m^2, the EQE drops from 28.6% measured for Dev 2 to 18.4% of Dev 4 with the spacer, as summarized in Table 1; Dev 4 maintains a constant EQE up to 1000 cd/m^2 with a value of 18.6% showing that the device still possesses a good charge balance with the turn-on voltage unaffected by the 1 nm 26DCzPPy layer. In Figure 3c, it is shown that at 1000 cd/m^2, no exciplex emission is visible in the EL spectrum, indicating that, all exciplexes produced at the 26DCzPPy:PO-T2T interface are transferred via FRET to the dopant, since the DET has been greatly reduced by the spacer layer separation. On the other hand, in Figure 4d, at a brightness of 10 000 cd/m^2, the exciplex emission is again clearly visible, at the same spectral position as that observed for Dev 1. The exciplex emission peaks at 471 nm, indicating the incomplete

DOI: 10.1021/acsami.8b15942
ACS Appl. Mater. Interfaces 2018, 10, 40001−40007

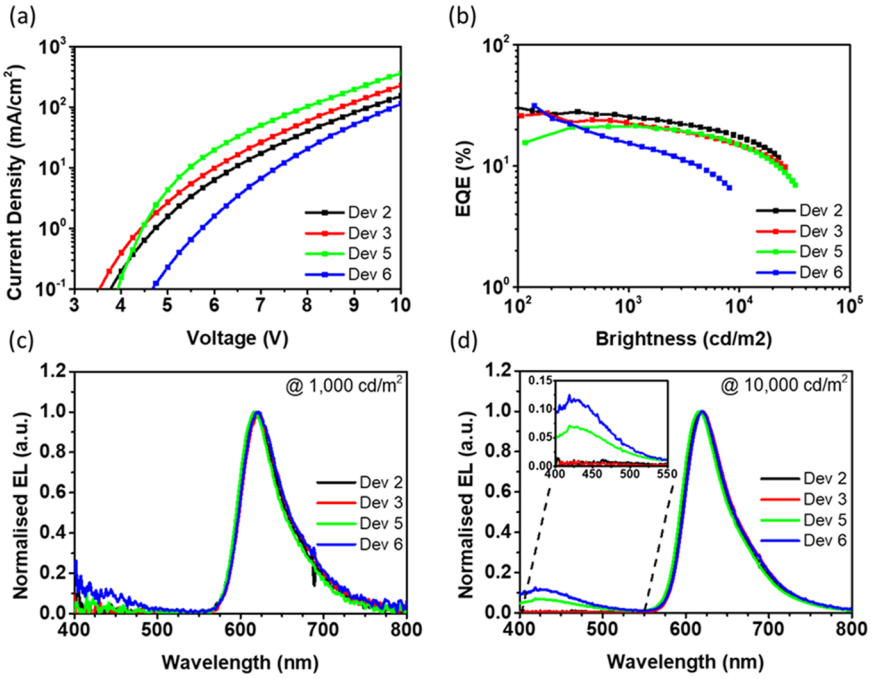

Figure 4. (a) *JV* and (b) EQE curves of the PhOLEDs with BCP and TPBi as the ETL and a 1 nm spacer between the EML and PO-T2T. Normalized EL spectra of the PhOLEDs at constant brightness of (c) 1000 cd/m^2 and (d) 10 000 cd/m^2.

energy transfer from the interfacial exciplex to the dopant. On the basis of the assumption that the 1 nm spacer layer does not affect the FRET efficacy and that DET must have been substantially eliminated,[26] we attribute the difference in efficiency between the devices with and without the spacer to the effective suppression of the DET contribution. Thus, the exciplex emission appears at high brightness even at 4 wt % doped EML. This indicates that the process of energy transfer from the interfacial exciplex to the dopant must be maximized to optimize the device efficiency.

PO-T2T was then replaced with two standard electron transport materials, TPBi and BCP. TPBi was chosen due to the very good LUMO alignment with 26DCzPPy, with a ΔE_{LUMO} = 0.14 eV.[27,28] BCP, on the other hand, was chosen because it has LUMO energy very similar to that of PO-T2T.[29,30] Despite having the same LUMO level as PO-T2T, BCP does not produce exciplex emission when blended with 26DCzPPy and neither does TPBi (Figures S3 and S4).

In Figure 4 are shown the results for the PhOLEDs with the structures NPB (40 nm)|TCTA (10 nm)|26DCzPPy (5 nm)|4 wt% of Ir(dmpq)$_2$acac in 26DCzPPy (5 nm)|TPBi (50 nm)| LiF (1 nm)|Al (100 nm) and NPB (40 nm)|TCTA (10 nm)| 26DCzPPy (5 nm)|7 wt% of Ir(dmpq)$_2$acac in 26DCzPPy (5 nm)|BCP (50 nm)|LiF (1 nm)|Al (100 nm), respectively, labeled as Dev 5 and Dev 6. Dev 5 shows lower performance with respect to that of the exciplex-enhanced devices, with good roll-off and EQE of 21.3% at 1000 cd/m^2, as in Table 1. The most interesting aspect is the substantial difference between the EQE obtained for the same doping level of 4 wt %, at 100 cd/m^2. The device where TPBi (Dev 5) is used shows a built-in efficiency with the EQE at 100 cd/m^2 as only 15.6% compared with 28.6% for Dev 2. The good resistance to roll-off is provided by the good energy level alignment with the bipolar host 26DCzPPy that guarantees the balance of the charges in the EML. On the other hand, the resulting performance is lower due to the absence of the energy transfer as well as a recombination zone localization effect arising from the TADF exciplex. Evidence of this is provided by comparing the EL spectra of the devices in Figure 4c,d. At 1000 cd/m^2, only the emission from the Ir(dmpq)$_2$acac is observable whereas at 10 000 cd/m^2, emission from the adjacent layer of 26DCzPPy is clearly visible, demonstrating the broadening of the recombination zone with the increasing voltage in the absence of the TADF exciplex at the host−ETL interface.

The same mechanism occurs when BCP is used to replace PO-T2T. In this last case, due to the large electron injection barrier alongside the low conductivity of BCP itself,[31] the operational voltage increases substantially, as visible in Figure 4a; it increases from 4.3 V with the exciplex to 5.5 V at 100 cd/m^2. The difference becomes even bigger at a brightness of 1000 cd/m^2 passing from 5.5 V with the exciplex to 7 V with the BCP layer. On the other hand, when BCP is used, very high efficiency of 31.5% is found at 100 cd/m^2, outperforming all other devices assessed in this work (Figure 4b). We consider this to be the effect of the device structure used. We believe that at low voltage, the electrons pile up at the ETL−EML interface as they cannot easily overcome the injection barrier between the BCP and 26DCzPPy (0.34 eV) and are more likely to be directly injected into the Ir(dmpq)2acac. Once injected into the dopant, the electrons are well confined by the 5 nm 26DCzPPy undoped layer. The only possibility for the recombination is with the holes trapped by the dopant, giving rise at a very sharp emission onset at a very low current and thus resulting in extremely high efficiency thanks to the high PLQY of the Ir(dmpq)$_2$acac.[32] At higher voltage, the electrons possess enough potential energy to inject into the EML host, bypassing this initially very efficient mechanism and causing the efficacy to reduce, halving the EQE already at 1000 cd/m^2.

Among the devices produced for this study, the only one showing a detectable secondary emission in the EL spectrum at 1000 cd/m^2 (Figure 4c) is the device with BCP as ETL (Dev 6), confirming the earlier suggestion that, for this device, the

DOI: 10.1021/acsami.8b15942
ACS Appl. Mater. Interfaces 2018, 10, 40001−40007

electrons have enough potential energy to overcome the injection barrier into the host, which moves the recombination zone toward the undoped 26DCzPPy layer. This effect is seen to increase at 10 000 cd/m^2 where both TPBi and BCP show emission from the host at ≈425 nm. The host emission in the EL spectrum is redshifted by 33 nm from the PL (Figure S3) again due to partial reabsorption by the Ir complex. The secondary emission from the host is a clear sign of the lost confinement of charge recombination in the EML.

Finally, in Figure 5, we compare the stability of the devices obtained operating the OLEDs at constant current with an initial brightness of 1000 cd/m^2. When the exciplex interface is present in the device structure the lifetime increases monotonically with the concentration of the dopant. We go from an LT90 of <1 min at 1 wt % to ≈1 h at 4 wt % and ≈6 h for 10 wt %. We attribute this increment to the increase of efficacy of the energy-transfer process due to the presence of a greater number of dopant molecules, thus avoiding charge build-up and quenching at the interface and degradation of the exciplex itself. Interestingly, the behavior of the device with the 1 nm spacer layer (Dev 4) shows the same LT90 as that of the one without the spacer layer (Dev 2) but then, its decay rate accelerates, with LT50 of 13.5 h with the 1 nm spacer layer whereas the device without the spacers has an LT50 of 24 h. This difference in our opinion highlights the role of DET in reducing charge pile up, and thus degradation at the interface rapidly quenches DET. Moreover, PhOLEDs where BCP (Dev 6) and TPBi (Dev 5) were used showed LT90 of <1 and 8 min, respectively. We attribute the longer LT90 obtained by the TPBi device over the BCP one to the better confinement of the recombination zone, as shown from the EL spectra of Figure 4 and discussed above. This difference shows the importance of the presence of the interfacial exciplex. The exciplex reduces the charge pile up at the interface and the degradation mechanism associated with it. The interfacial exciplex turns the piled-up charges into useful light that is transferred to the Ir(dmpq)$_2$acac through FRET and DET. BCP device exhibits lower stability than TPBi due to the lost exciton confinement in the 5 nm thick EML, spreading the recombination zone in nonefficient areas of the device, i.e., the undoped host.

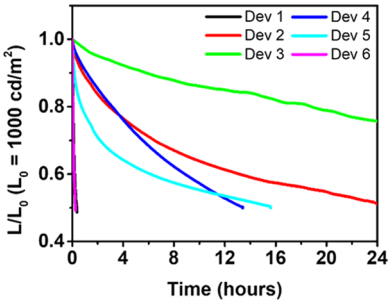

Figure 5. Luminance decay of the OLEDs measured at constant current. All devices are kept at the current value that corresponds to the initial luminance L_0 = 1000 cd/m^2.

CONCLUSIONS

We successfully demonstrated that utilizing a TADF exciplex at the interface between EML and ETL can improve the efficiency and stability of OLEDs. We highlight this improvement as a consequence of an extremely effective localization of the excitons into the 5 nm EML. The interfacial exciplex not only localizes the recombination zone onto the EML−ETL interface but also harvests the holes and electrons piled up at that interface, forming exciplexes and recycling them into useful light in the emitter. We show clearly that both DET and FRET mechanisms are responsible for the energy-transfer process from the exciplex to the dopant and that the DET process provides a very important contribution to the overall efficiency of the devices. Using the TADF exciplex interface layer on the electron side of the device greatly increases device lifetime LT90 from minutes to hours at 1000 cd/m^2. In future, this strategy can be promising for implementation in hyperfluorescent OLEDs for further improving the energy-transfer mechanisms and boosting the efficiency.

ASSOCIATED CONTENT

Supporting Information

The Supporting Information is available free of charge on the ACS Publications website at DOI: 10.1021/acsami.8b15942.

Photoluminescence decay with biexponential fit at 295 K; 295 and 80 K time-resolved photoluminescence spectra of 26DCzPPy:PO-T2T exciplex; photoluminescence spectra of 26DCzPPy, TPBi, and 26DCzPPy:TPBi blend; photoluminescence spectra of 26DCzPPy, BCP, and 26DCzPPy:BCP blend (PDF)

AUTHOR INFORMATION

Corresponding Author

*E-mail: marco.colella@durham.ac.uk.

ORCID

Marco Colella: 0000-0003-1627-2978
Piotr Pander: 0000-0003-4103-4154
Daniel de Sa Pereira: 0000-0002-5784-2124
Andrew P. Monkman: 0000-0002-0784-8640

Notes

The authors declare no competing financial interest.

ACKNOWLEDGMENTS

The authors would like to acknowledge the EXCILIGHT project funded by the European Union's Horizon 2020 Research and Innovation Program under grant agreement No. 674990.

REFERENCES

(1) Tang, C. W.; VanSlyke, S. A. Organic Electroluminescent Diodes. *Appl. Phys. Lett.* **1987**, *51*, 913.

(2) Baldo, M. A.; O'Brien, D. F.; You, Y.; Shoustikov, A.; Sibley, S.; Thompson, M. E.; Forrest, S. R. Highly Efficient Phosphorescent Emission from Organic Electroluminescent Devices. *Nature* **1998**, *395*, 151−154.

(3) Uoyama, H.; Goushi, K.; Shizu, K.; Nomura, H.; Adachi, C. Highly Efficient Organic Light-Emitting Diodes from Delayed Fluorescence. *Nature* **2012**, *492*, 234−238.

(4) Dias, F. B.; Penfold, T. J.; Monkman, A. P. Photophysics of Thermally Activated Delayed Fluorescence Molecules. *Methods Appl. Fluoresc.* **2017**, *5*, No. 012001.

(5) Dos Santos, P. L.; Dias, F. B.; Monkman, A. P. Investigation of the Mechanisms Giving Rise to TADF in Exciplex States. *J. Phys. Chem. C* **2016**, *120*, 18259−18267.

(6) Kondakova, M. E.; Pawlik, T. D.; Young, R. H.; Giesen, D. J.; Kondakov, D. Y.; Brown, C. T.; Deaton, J. C.; Lenhard, J. R.; Klubek, K. P. High-Efficiency, Low-Voltage Phosphorescent Organic Light-

DOI: 10.1021/acsami.8b15942
ACS Appl. Mater. Interfaces 2018, 10, 40001−40007

Emitting Diode Devices with Mixed Host. *J. Appl. Phys.* **2008**, *104*, No. 094501.
(7) Fukagawa, H.; Shimizu, T.; Kamada, T.; Kiribayashi, Y.; Osada, Y.; Hasegawa, M.; Morii, K.; Yamamoto, T. Highly Efficient and Stable Phosphorescent Organic Light-Emitting Diodes Utilizing Reverse Intersystem Crossing of the Host Material. *Adv. Opt. Mater.* **2014**, *2*, 1070−1075.
(8) Fukagawa, H.; Shimizu, T.; Kamada, T.; Yui, S.; Hasegawa, M.; Morii, K.; Yamamoto, T. Highly Efficient and Stable Organic Light-Emitting Diodes with a Greatly Reduced Amount of Phosphorescent Emitter. *Sci. Rep.* **2015**, *5*, No. 9855.
(9) Fukagawa, H.; Shimizu, T.; Iwasaki, Y.; Yamamoto, T. Operational Lifetimes of Organic Light-Emitting Diodes Dominated by Förster Resonance Energy Transfer. *Sci. Rep.* **2017**, *7*, No. 1735.
(10) Park, Y.-S.; Lee, S.; Kim, K.-H.; Kim, S.-Y.; Lee, J.-H.; Kim, J.-J. Exciplex-Forming Co-Host for Organic Light-Emitting Diodes with Ultimate Efficiency. *Adv. Funct. Mater.* **2013**, *23*, 4914−4920.
(11) Lee, S.; Koo, H.; Kwon, O.; Jae Park, Y.; Choi, H.; Lee, K.; Ahn, B.; Min Park, Y. The Role of Charge Balance and Excited State Levels on Device Performance of Exciplex-Based Phosphorescent Organic Light Emitting Diodes. *Sci. Rep.* **2017**, *7*, No. 11995.
(12) Duan, L.; Hou, L.; Lee, T.-W.; Qiao, J.; Zhang, D.; Dong, G.; Wang, L.; Qiu, Y. Solution Processable Small Molecules for Organic Light-Emitting Diodes. *J. Mater. Chem.* **2010**, *20*, 6392−6407.
(13) Zhang, D.; Cai, M.; Zhang, Y.; Bin, Z.; Zhang, D.; Duan, L. Simultaneous Enhancement of Efficiency and Stability of Phosphorescent OLEDs Based on Efficient Förster Energy Transfer from Interface Exciplex. *ACS Appl. Mater. Interfaces* **2016**, *8*, 3825−3832.
(14) Zhao, B.; Zhang, T.; Chu, B.; Li, W.; Su, Z.; Wu, H.; Yan, X.; Fangming, J.; Gao, Y.; Chengyuan, L. Highly Efficient Red OLEDs Using DCJTB as the Dopant and Delayed Fluorescent Exciplex as the Host. *Sci. Rep.* **2015**, *5*, No. 10697.
(15) Sarma, M.; Wong, K. T. Exciplex: An Intermolecular Charge-Transfer Approach for TADF. *ACS Appl. Mater. Interfaces* **2018**, *10*, 19279−19304.
(16) Zhang, D.; Duan, L.; Zhang, D.; Qiu, Y. Towards Ideal Electrophosphorescent Devices with Low Dopant Concentrations: The Key Role of Triplet up-Conversion. *J. Mater. Chem. C* **2014**, *2*, 8983−8989.
(17) Liu, X.-K.; Chen, W.; Thachoth Chandran, H.; Qing, J.; Chen, Z.; Zhang, X.-H.; Lee, C.-S. High-Performance, Simplified Fluorescence and Phosphorescence Hybrid White Organic Light-Emitting Devices Allowing Complete Triplet Harvesting. *ACS Appl. Mater. Interfaces* **2016**, *8*, 26135−26142.
(18) Dias, F. B.; Penfold, T. J.; Monkman, A. P. Photophysics of Thermally Activated Delayed Fluorescence Molecules. *Methods Appl. Fluoresc.* **2017**, *5*, No. 012001.
(19) Su, S.-J.; Sasabe, H.; Takeda, T.; Kido, J. Pyridine-Containing Bipolar Host Materials for Highly Efficient Blue Phosphorescent OLEDs. *Chem. Mater.* **2008**, *20*, 1691−1693.
(20) Gong, X.; Ostrowski, J. C.; Moses, D.; Bazan, G. C.; Heeger, A. J. Electrophosphorescence from a Polymer Guest-Host System with an Iridium Complex as Guest: Förster Energy Transfer and Charge Trapping. *Adv. Funct. Mater.* **2003**, *13*, 439−444.
(21) Lin, W.; Huang, W.; Huang, M.; Fan, C.; Lin, H.-W.; Chen, L.-Y.; Liu, Y.-W.; Lin, J.-S.; Chao, T.-C.; Tseng, M.-R. A Bipolar Host Containing Carbazole/Dibenzothiophene for Efficient Solution-Processed Blue and White Phosphorescent OLEDs. *J. Mater. Chem. C* **2013**, *1*, 6835−6841.
(22) Jeon, S. O.; Yook, K. S.; Joo, C. W.; Lee, J. Y. Phenylcarbazole-Based Phosphine Oxide Host Materials For High Efficiency In Deep Blue Phosphorescent Organic Light-Emitting Diodes. *Adv. Funct. Mater.* **2009**, *19*, 3644−3649.
(23) Song, D.; Zhao, S.; Luo, Y.; Aziz, H. Causes of Efficiency Roll-off in Phosphorescent Organic Light Emitting Devices: Triplet-Triplet Annihilation versus Triplet-Polaron Quenching. *Appl. Phys. Lett.* **2010**, *97*, No. 243304.
(24) Al Attar, H. A.; Monkman, A. P. Electric Field Induce Blue Shift and Intensity Enhancement in 2D Exciplex Organic Light Emitting Diodes; Controlling Electron-Hole Separation. *Adv. Mater.* **2016**, *28*, 8014−8020.
(25) O'Brien, D. F.; Baldo, M. A.; Thompson, M. E.; Forrest, S. R. Improved Energy Transfer in Electrophosphorescent Devices. *Appl. Phys. Lett.* **1999**, *74*, 442.
(26) Luhman, W. A.; Holmes, R. J. Investigation of Energy Transfer in Organic Photovoltaic Cells and Impact on Exciton Diffusion Length Measurements. *Adv. Funct. Mater.* **2011**, *21*, 764−771.
(27) Cai, C.; Su, S.; Chiba, T.; Sasabe, H.; Pu, Y.; Nakayama, K.; Kido, J. High-Efficiency Red , Green and Blue Phosphorescent Homojunction Organic Light-Emitting Diodes Based on Bipolar Host Materials. *Org. Electron.* **2011**, *12*, 843−850.
(28) Jankus, V.; Chiang, C. J.; Dias, F.; Monkman, A. P. Deep Blue Exciplex Organic Light-Emitting Diodes with Enhanced Efficiency; P-Type or E-Type Triplet Conversion to Singlet Excitons? *Adv. Mater.* **2013**, *25*, 1455−1459.
(29) Adamovich, V.; Brooks, J.; Tamayo, A.; Alexander, A. M.; Djurovich, P. I.; Andrade, B. W. D.; Adachi, C.; Forrest, R.; Thompson, M. E. High Efficiency Single Dopant White Electrophosphorescent Light Emitting Diodes. *New J. Chem.* **2002**, *26*, 1171−1178.
(30) Hung, W. Y.; Fang, G. C.; Lin, S. W.; Cheng, S. H.; Wong, K. T.; Kuo, T. Y.; Chou, P. T. The First Tandem, All-Exciplex-Based Woled. *Sci. Rep.* **2014**, *4*, No. 5161.
(31) Wu, I. W.; Wang, P. S.; Tseng, W. H.; Chang, J. H.; Wu, C. I. Correlations of Impedance-Voltage Characteristics and Carrier Mobility in Organic Light Emitting Diodes. *Org. Electron.* **2012**, *13*, 13−17.
(32) Kim, D. H.; Cho, N. S.; Oh, H. Y.; Yang, J. H.; Jeon, W. S.; Park, J. S.; Suh, M. C.; Kwon, J. H. Highly Efficient Red Phosphorescent Dopants in Organic Light-Emitting Devices. *Adv. Mater.* **2011**, *23*, 2721−2726.

DOI: 10.1021/acsami.8b15942
ACS Appl. Mater. Interfaces 2018, 10, 40001−40007